BI-TP 97/34
WUE-ITP-97-034
MPI-PhE/97-23

BI-TP 97/34
WUE-ITP-97-034
MPI-PhE/97-23

hep-ph/9709315

hep-ph/9709315 11 Sep 1997

Leptoquark Pair Production at e^+e^- Linear Colliders: Signals and Background

R. Rückl[1,2], R. Settles[2] and H. Spiesberger[3]

[1] *Institut für Theoretische Physik, Universität Würzburg, D-97074 Würzburg, Germany*

[2] *Max-Planck-Institut für Physik, Werner-Heisenberg-Institut, D–80805 München, Germany*

[4] *Fakultät für Physik, Universität Bielefeld, D-33501 Bielefeld, Germany*

September 11, 1997

ABSTRACT

We study pair production of leptoquarks in e^+e^- annihilation at linear colliders. A detailed simulation including beamstrahlung and initial state radiation, leptoquark decay and hadronization, as well as detector smearing, is performed. Discovery limits are estimated for center-of-mass energies of 500 and 800 GeV. The prospects for determining masses and couplings of leptoquarks are also investigated.

To appear in the Proceedings of the *Joint ECFA/DESY Study on Physics and Detectors for the Linear Collider*, February to November 1996, ed. R. Settles, DESY 97-123E.

1 Introduction

Leptoquarks appear in extensions of the standard model involving unification, technicolor, compositeness, or R-parity violating supersymmetry. Hence, the search for leptoquarks is an important task at present and future high energy experiments. Furthermore, leptoquark pair production leads to novel experimental signatures involving fixed-mass lepton-jet systems, and thus provides an interesting example for detector studies.

In e^+e^- annihilation, pair production of scalar leptoquarks by s-channel γ and Z exchange is uniquely determined by gauge symmetry if one assumes minimal couplings, while vector leptoquarks may also possess anomalous couplings. In addition to s-channel production, there are t-channel processes involving unknown Yukawa couplings. Similarly, pair production of leptoquarks at hadron colliders is determined by the QCD gauge couplings with contributions from anomalous and Yukawa couplings. In contrast, in lepton-nucleon scattering the dominant s-channel leptoquark production, as well as t- and u-channel scattering, proceeds via Yukawa couplings only.

In the generally adopted framework described in Ref. [1], the Yukawa couplings are taken to be dimensionless and $SU(3) \times SU(2) \times U(1)$ symmetric. Moreover, they are assumed to conserve lepton- and baryon-number in order to avoid rapid proton decay, to be non-zero only within one family in order to exclude FCNC processes beyond the CKM mixing, and chiral in order to avoid the very strong bounds from leptonic pion decays. The allowed states can be classified according to spin, weak isospin and fermion number. They are summarized in Table 1.

The leptoquark masses and couplings are constrained by high-energy data. Direct searches for leptoquarks have been performed at the Tevatron, at HERA and at LEP. Recently, both experiments, CDF and D0, have improved their mass limits for scalar leptoquarks considerably. D0 excludes first generation leptoquarks with masses below 225 GeV assuming a branching ratio $B_{eq} = 1$ for decays into electrons [2], whereas CDF quotes a limit of 213 GeV [3] (all mass limits are at 95 % CL). For branching ratios less than one, the limits are weaker, e.g., $M > 176$ GeV for $B_{eq} = 0.5$ [2]. The bounds on vector states are even stronger: 298 GeV for $B_{eq} = 1$ and 270 GeV for $B_{eq} = 0.5$ [4]. The corresponding bounds on second and third generation scalar leptoquarks are $M > 184$ GeV for $B_{\mu q} = 1$ and $M > 98$ GeV for $B_{\tau q} = 1$, respectively [5]. The LHC is expected to reach the TeV range. Mass limits obtained at HERA depend on the Yukawa couplings $\lambda_{L,R}$. They range from 207 to 272 GeV for $\lambda_{L,R} = e$ [6] where e is the electromagnetic coupling strength . The precise mass limit also varies with the type of leptoquark specified in Table 1. The above limits are lowered by about 50 GeV if $\lambda_{L,R} = 0.1$. Finally, the most stringent but $\lambda_{L,R}$-dependent limit from LEP originates from the search for single-leptoquark production and excludes masses below 131 GeV assuming $\lambda_{L,R} > e$ [7]. The mass bounds from leptoquark pair production roughly reach $\sqrt{s}/2$ [8], $\sqrt{s}$ being the center-of-mass energy, and are thus much weaker than the Tevatron bounds.

Indirect bounds on Yukawa couplings and masses can be derived from low-energy data [9]. For chiral couplings, the most restrictive limits come from atomic parity violation

	State	${}^{Q}\bar{\Phi}_T$	$\lambda_{L,R}$	Channel	Limits	$g_1(s)$	$\sigma_{tot}(s)$[fb]
1	S_1	${}^{-1/3}S_0$	g_L g_R $-g_L$	$e^-_L u_L$ $e^-_R u_R$ $\nu_e d_L$	$g_L < 0.06$ $g_R < 0.1$	0.236	6.15
2	$\tilde{S}_1$	${}^{-4/3}\tilde{S}_0$	g_R	$e^-_R d_R$	$g_R < 0.1$	3.77	98.2
3	S_3	${}^{+2/3}S_1$ ${}^{-1/3}S_1$ ${}^{-4/3}S_1$	$\sqrt{2}g_L$ $-g_L$ $-g_L$ $-\sqrt{2}g_L$	$\nu_e u_L$ $\nu_e d_L$ $e^-_L u_L$ $e^-_L d_L$	$g_L < 0.09$	4.23 0.236 6.05	110 6.15 158
4	R_2	${}^{-2/3}S_{1/2}$ ${}^{-5/3}S_{1/2}$	g_L $-g_R$ g_L g_R	$\nu_e \bar{u}_L$ $e^-_R \bar{d}_R$ $e^-_L \bar{u}_L$ $e^-_R \bar{u}_R$	$g_L < 0.1$ $g_R < 0.09$	2.52 5.70	65.8 149
5	$\tilde{R}_2$	${}^{+1/3}\tilde{S}_{1/2}$ ${}^{-2/3}\tilde{S}_{1/2}$	g_L g_L	$\nu_e \bar{d}_L$ $e^-_L \bar{d}_L$	$g_L < 0.1$	1.06 1.51	27.6 39.5
6	V_2	${}^{-1/3}V_{1/2}$ ${}^{-4/3}V_{1/2}$	g_L g_R g_L g_R	$\nu_e d_R$ $e^-_R u_L$ $e^-_L d_R$ $e^-_R d_L$	$g_L < 0.09$ $g_R < 0.05$	1.56 3.84	365 895
7	$\tilde{V}_2$	${}^{+2/3}\tilde{V}_{1/2}$ ${}^{-1/3}\tilde{V}_{1/2}$	g_L g_L	$\nu_e u_R$ $e^-_L u_R$	$g_L < 0.09$	1.51 1.06	353 247
8	U_1	${}^{-2/3}V_0$	g_L g_R g_L	$e^-_L \bar{d}_R$ $e^-_R \bar{d}_L$ $\nu_e \bar{u}_R$	$g_L < 0.05$ $g_R < 0.09$	0.942	222
9	$\tilde{U}_1$	${}^{-5/3}\tilde{V}_0$	g_R	$e^-_R \bar{u}_L$	$g_R < 0.09$	5.89	1370
10	U_3	${}^{+1/3}V_1$ ${}^{-2/3}V_1$ ${}^{-5/3}V_1$	$\sqrt{2}g_L$ $-g_L$ g_L $\sqrt{2}g_L$	$\nu_e \bar{d}_R$ $e^-_L \bar{d}_R$ $\nu_e \bar{u}_R$ $e^-_L \bar{u}_R$	$g_L < 0.04$	4.02 0.942 7.67	942 222 1790

Table 1: *Properties of leptoquarks. Columns 2 and 3 show the notations of Refs. [1] and [12], respectively. The upper half of the Table refers to scalars, the lower to vectors. The lower indices denote the weak isospin, multiplicity $2T+1$ or total isospin T. The upper index is the electromagnetic charge. The Yukawa couplings $g_{L,R}$ are as defined in Ref. [1], while $\lambda_{L,R}$ is used as a generic symbol. Column 5 specifies the production and decay channels, while the low-energy limits on the Yukawa couplings from Ref. [9] for $M = 200$ GeV are given in column 6. The last two columns quantify the effective coupling $g_1(s)$ defined in Eq. (6) and the total cross section $\sigma_{tot}(s)$ given in Eqs. (11, 12) taking $\sqrt{s} = 500$ GeV, $M = 200$ GeV, $g_L = g_R = 0$, and including corrections due to beamstrahlung and initial state radiation.*

and lepton and quark universality. The maximum allowed couplings for $M = 200$ GeV and first generation leptoquarks are given in Table 1 [10].

The present work extends previous studies [11] in several ways:

(i) complete simulation of leptoquark production and decay

$$e^+e^- \to \Phi\bar{\Phi} \to l_1 q_1 \bar{l}_2 \bar{q}_2 \quad \text{or} \quad l_1 \bar{q}_1 \bar{l}_2 q_2, \tag{1}$$

taking into account beamstrahlung, initial-state radiation and quark hadronization;

(ii) simulation of the main background processes

$$e^+e^- \to WW, \quad ZZ, \tag{2}$$

$$e^+e^- \to l_1 \bar{l}_2 q_3 \bar{q}_4, \tag{3}$$

$$e^+e^- \to \bar{t}t; \tag{4}$$

(iii) inclusion of acceptance and smearing effects for different detector models.

After the presentation of calculational details in section 2 and experimental considerations in section 3, the results on detection efficiencies and sensitivity limits are discussed in section 4.

2 Theoretical Framework

In e^+e^- annihilation, leptoquarks can be pair-produced via photon and Z boson s-channel exchange and via t-channel exchange of quarks. The couplings of leptoquarks to gauge bosons are given in Ref. [13][1], the couplings to fermions in Ref. [1]. With these couplings, the differential cross section for the production of scalar or vector leptoquarks of mass M is given by [13]

$$\frac{d\hat{\sigma}}{d\cos\theta} = \frac{3\pi\alpha^2}{8} N \left\{ \sin^2\theta \left[A_0 + \frac{A_1}{t} + \frac{A_2}{t^2} \right] + B_0 + \frac{B_1}{t} \right\}, \tag{5}$$

where $t = 1 + \beta^2 - 2\beta\cos\theta$ with $\beta = \sqrt{1 - 4M^2/s}$. The coefficients N, A_i and B_i are listed in Table 2, the effective coupling parameters g_i being defined by

$$g_1 = \sum_{a=L,R} |\kappa_a(s)|^2 \tag{6}$$

$$g_2 = 4 \sum_{a=L,R} \left(\frac{\lambda_a}{e} \right)^2 \mathrm{Re}\kappa_a(s) \tag{7}$$

[1]For a generalization including anomalous couplings of vector states, see Ref. [14]. The couplings to gauge bosons used here correspond to minimal couplings with $\kappa = 1$ and $\lambda = 0$.

$$g_3 = 4 \sum_{a=L,R} \left(\frac{\lambda_a}{e} \right)^4 \tag{8}$$

with

$$\kappa_a(s) = \sum_{V=\gamma,Z} Q_a^V(e) \frac{s}{s - M_V^2 + iM_V\Gamma_V} Q^V(\Phi), \tag{9}$$

and λ_a denoting the Yukawa couplings specified in Table 1. In the above, $e = \sqrt{4\pi\alpha}$, $M_\gamma = \Gamma_\gamma = 0$, and M_Z and Γ_Z are the mass and the width of the Z boson, respectively. The electron and leptoquark electroweak charges are given by

$$\begin{aligned} &Q_{L,R}^\gamma(e) = -1, \quad Q_L^Z(e) = \frac{-1/2 + s_w^2}{s_w c_w}, \quad Q_R^Z(e) = \frac{s_w}{c_w}, \\ &Q^\gamma(\Phi) = Q, \qquad Q^Z(\Phi) = \frac{T_3 - Q s_w^2}{c_w s_w} \end{aligned} \tag{10}$$

where Q is the electric charge in units of e, T_3 the third component of the weak isospin, and s_w (c_w) the sine (cosine) of the weak mixing angle.

	scalar	vector
N	$\frac{\beta^3}{s}$	$\frac{\beta}{M^2}$
A_0	g_1	$\frac{1}{4}\beta^2(1-3\beta^2)g_1 - \frac{1}{4}\beta^2 g_2 + \frac{\beta^2 s}{16M^2} g_3$
A_1	g_2	$\frac{1}{2}\beta^2(1-\beta^2)g_2$
A_2	g_3	$\beta^2(1-\beta^2)g_3$
B_0	0	$\beta^2 g_1 + \frac{1}{2}(1+\beta^2)g_2 + g_3$
B_1	0	$-\frac{1}{2}(1-\beta^2)^2 g_2$

Table 2: *Coefficients appearing in the cross section formula Eq. (5).*

The total cross section can be written in the following form [13, 14]:

$$\hat{\sigma} = \frac{\pi\alpha^2}{2} N \left(F_1^J g_1 + F_2^J g_2 + F_3^J g_3 \right) \tag{11}$$

using the same effective couplings g_i, $i = 1, 2, 3$ defined in Eqs. (6, 7, 8) and

$$\begin{aligned}
F_1^S &= 1, \\
F_2^S &= \frac{3}{8}\left(\frac{1+\beta^2}{\beta^2} - \frac{(1-\beta^2)^2}{2\beta^3}\ln\frac{1+\beta}{1-\beta}\right), \\
F_3^S &= \frac{3}{4}\left(-\frac{1}{\beta^2} + \frac{1+\beta^2}{2\beta^3}\ln\frac{1+\beta}{1-\beta}\right), \\
F_1^V &= \beta^2\frac{7-3\beta^2}{4}, \\
F_2^V &= \frac{15}{16} + \frac{1}{2}\beta^2 - \frac{3}{16}\beta^4 - \frac{3}{32\beta}\left(1-\beta^2\right)^2\left(5-\beta^2\right)\ln\frac{1+\beta}{1-\beta}, \\
F_3^V &= \frac{3}{4}\left(1+\beta^2\right) + \frac{\beta^2}{16}\frac{s}{M^2}\frac{3}{8\beta}\left(1-\beta^4\right)\ln\frac{1+\beta}{1-\beta}.
\end{aligned} \tag{12}$$

The normalization factor N is as given in Table 2. Asymptotically, for $M^2 \ll s$, the s-channel and the s/t-interference contributions scale like $1/s$ for scalar leptoquarks and approach constant values for vectors. The pure t-channel contribution scales with $\frac{1}{s}\ln(s/M^2)$ for scalars, but grows like s/M^4 for vectors. The latter behavior eventually leads to unitarity violation and thus indicates that the effective Lagrangian from which the above cross section formulae have been derived has to be embedded into a more fundamental theory at high energies. However, for Yukawa couplings obeying the experimental bounds of Table 1 this problem only arises far beyond the energy range considered here.

At high-luminosity e^+e^- colliders, beamstrahlung leads to a significant energy spread in the electron and positron beams. This effect can be described with the help of a radiator function $G_{e^+e^-}(x_+, x_-, s)$ where $x_\pm$ is related to the fractional energy loss, $E_\pm = x_\pm\sqrt{s}/2$. The transverse momentum spread of the beam due to beamstrahlung can be neglected. Therefore, the cross sections including the effect of beamstrahlung can be obtained from Eqs. (5) and (11) by a simple convolution:

$$d\sigma_{bs}(s) = \int dx_+ dx_- d\hat{\sigma}(x_+x_-s)G_{e^+e^-}(x_+, x_-, s). \tag{13}$$

Because of singularities at the end-points $x_+ = 1$ and $x_- = 1$, $G_{e^+e^-}(x_+, x_-)$ is split into δ-function terms (the probability for no energy loss by beamstrahlung) and a smooth function of x_+ and x_-. The radiator function depends on machine parameters and is numerically provided by the program `circe` [15].

The most important QED correction arises from initial state radiation (ISR). The universal part of this effect can again be described by a radiator function[2]:

$$D_{e/e}(z) = \delta(1-z)\left[1 + \frac{\alpha}{2\pi}\ln\frac{4E^2}{m_e^2}\left(2\ln\epsilon + \frac{3}{2}\right)\right] + \theta(1-z-\epsilon)\frac{\alpha}{2\pi}\frac{1+z^2}{1-z}\ln\frac{4E^2}{m_e^2} \tag{14}$$

[2] $D_{e/e}$ is actually known up to $O(\alpha^2)$, but since the non-universal contributions to $O(\alpha)$ are not known for the process under consideration, we also do not include the $O(\alpha^2)$ effects in $D_{e/e}$.

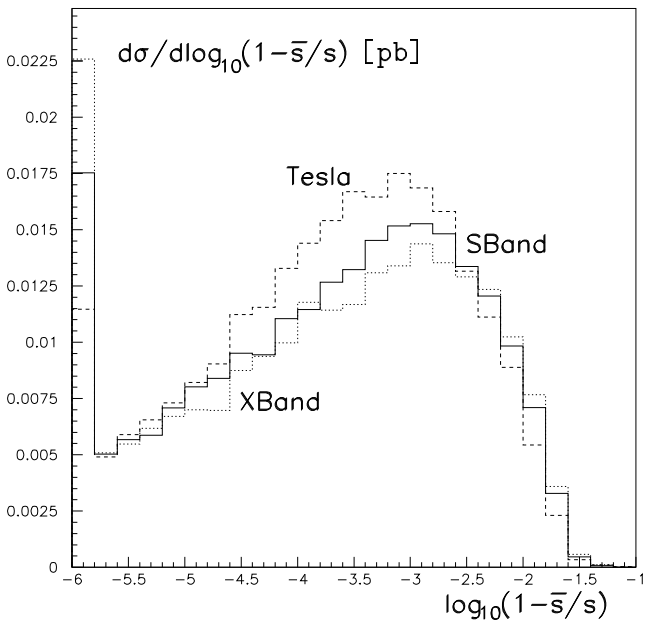

Figure 1: *Distribution of the production cross section in the effective collision energy* $\sqrt{\bar{s}}$ *for the scalar leptoquark* ${}^{-4/3}S_1$. *The three histograms refer to the Tesla (dashed), S-Band (full) and X-Band (dotted) options for* $\sqrt{s} = 500$ *GeV,* $M = 200$ *GeV,* $\lambda_L = \lambda_R = 0$.

where E is the beam energy. The parameter ϵ is a photon energy cutoff separating soft from hard photons. The δ-function term includes soft bremsstrahlung where photons have an energy $E_\gamma < \epsilon E$. The second term proportional to the θ-function describes the emission of photons with $E_\gamma > \epsilon E$. Similarly as in Eq. (13), the corrected cross section follows by convolution:

$$d\sigma = \int_0^1 dz D_{e/e}(z) d\hat{\sigma}(zE_+, E_-) + \int_0^1 dz D_{e/e}(z) d\hat{\sigma}(E_+, zE_-). \tag{15}$$

In addition, for s-channel diagrams, higher-order corrections due to vacuum polarization can be included by using the running fine-structure constant [16].

If one wants to take into account beamstrahlung simultaneously with ISR, one has to substitute in Eq. (15) $d\hat{\sigma}$ by $d\sigma_{bs}$ given in Eq. (13) and E_+ (E_-) by $x_+\sqrt{s}/2$ ($x_-\sqrt{s}/2$). The reduced center-of-mass energy squared after beamstrahlung and ISR is given by $\bar{s} = x_+ x_- z s$. The separation of $G_{e^+e^-}$ and $D_{e/e}$ into δ-function terms and smooth functions and the distinction of initial-state radiation from electrons and positrons requires to compute eight separate contributions to the cross sections. Technically, the mapping $z \to \ln(1-z)$ leads to numerically stable integration.

Presently, three different options for the beam dynamics of an e^+e^- collider are being discussed. The differences in the distributions of the cross sections in $\bar{s}$ are exemplified in Fig. 1 for the leptoquark ${}^{-4/3}S_1$ having the largest cross section. For the present study, we choose the Tesla option. The bulk of the events is accompanied by soft radiation with

a maximum at $1 - \bar{s}/s \simeq 10^{-3}$, but with a tail extending to a few percent. This limits the possibility to reconstruct the kinematics of final states with missing momentum by imposing the constraints of energy-momentum conservation.

QCD corrections are not taken into account in our calculations. They are known only for the total cross section of scalar leptoquark production [17]. The correction factor $\delta_s = 1 + \alpha_s F(\beta)$ is shown in Fig. 2. At $\beta \leq 0.2$ the corrections exceed 100 %. In this region close to the threshold it will certainly be necessary to take into account bound state dynamics. At large β, one expects corrections of the order of 20 % which increase the cross section.

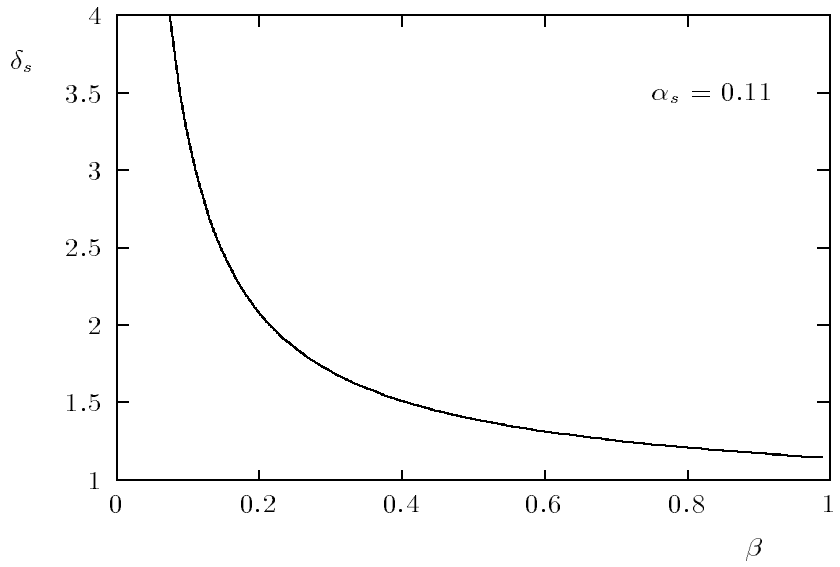

Figure 2: *QCD correction factor δ_s for the total production cross section of scalar leptoquarks as a function of β.*

In Fig. 3, finally, we illustrate the effects due to beamstrahlung and ISR on the integrated cross sections for representative scalar and vector leptoquarks. Except for scalars at very high $\sqrt{s}$, the total cross section is reduced typically by 10 %: 1 to 2 fb for scalars and 60 fb for vectors. The reduction is particularly important for the discovery reach near threshold.

Figure 4 shows the total cross section for leptoquark pair-production at two center-of-mass energies and for those species of scalar and vector leptoquarks which have the minimal and maximal cross sections in each class. From the figure it is clear that, given the mass, the measurement of the total cross section already provides an important piece of information on the type of the leptoquark produced. As demonstrated later, another important observable is the angular distribution.

Additional information can be inferred from decay properties. They are determined by the Yukawa couplings. The partial decay widths per channel (see Table 1) are given

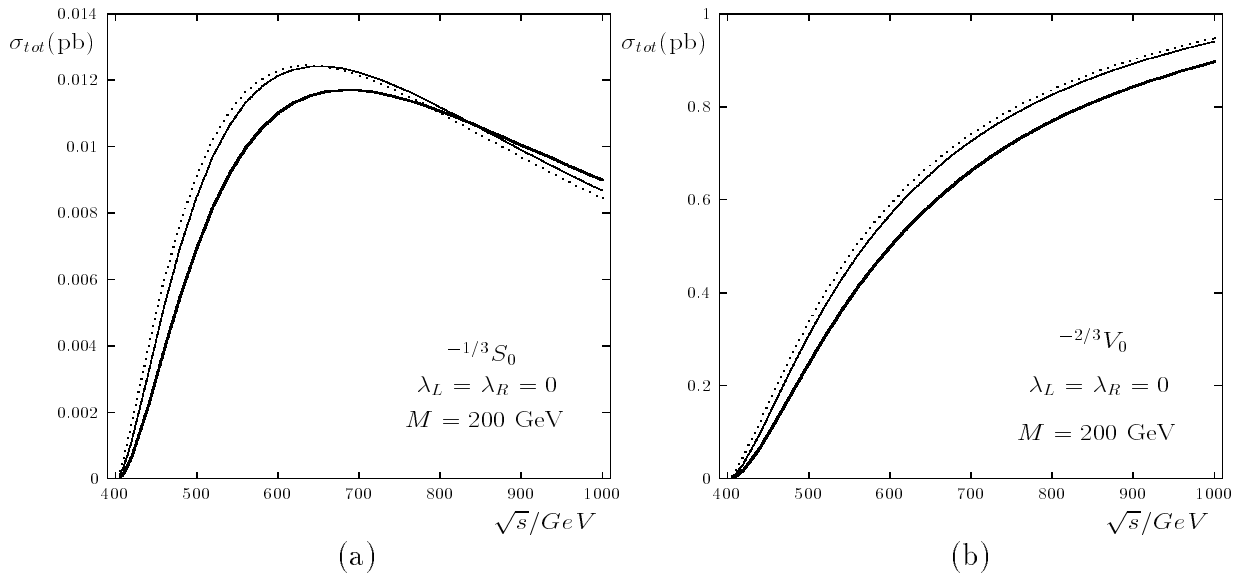

Figure 3: *Effects of beamstrahlung and initial state radiation on the pair-production cross sections for the $^{-1/3}S_0$ (a) and $^{-2/3}V_0$ (b) leptoquarks. The dotted curves are the Born cross sections, the thin full curves include beamstrahlung, and the thick full curves give the total cross section including both beamstrahlung and ISR.*

by [1]

$$\begin{aligned} \Gamma_S &= \frac{1}{16\pi^2}\lambda_{L,R}^2 M \qquad \text{for scalars,} \\ \Gamma_V &= \frac{1}{24\pi^2}\lambda_{L,R}^2 M \qquad \text{for vectors.} \end{aligned} \tag{16}$$

Quantitatively, for $M = 200$ GeV and $\lambda_{L,R} = e$ one has Γ_S (Γ_V) = 116 (77) MeV, i.e., very narrow states. Furthermore, for the leptoquarks considered here, the branching ratios B_{eq} for charged lepton channels and $B_{\nu q}$ for neutrino channels add up to unity, $B_{eq} + B_{\nu q} = 1$, with B_{eq} as given in Table 3. If one assumes that the members of a given isomultiplet of leptoquarks are almost mass-degenerate, one sees that the strongest bounds, $M \gtrsim 225$ GeV for scalars and $M \gtrsim 300$ GeV for vectors, obtained at the Tevatron for $B_{eq} = 1$ apply to all leptoquark species except the two singlets $^{-1/3}S_0$ and $^{-2/3}V_0$. The latter two may have branching fractions $1/2 \leq B_{eq} \leq 1$ so that only the weaker limits $M_{S_0} > 176$ GeV and $M_{V_0} > 270$ GeV hold. Note that for first generation leptoquarks in this mass range, B_{eq} must be very close to 1/2 ($r = 0$) or 1 ($r = \infty$) unless $\lambda_L \lambda_R \ll 1$. In more general scenarios where leptoquarks have additional decay channels, as is the case for example for squarks in supersymmetric models with R-parity violation, B_{eq} and $B_{\nu q}$ are not fixed by the Yukawa couplings alone. They rather can be considered as independent parameters leading to more model-dependent mass bounds. We also mention the possibility for generic leptoquarks to have tiny Yukawa couplings and hence being very long-lived. In this case, they would have to form bound states (leptohadrons) which do not decay inside the detector. This requires special search strategies, e.g., for fractional

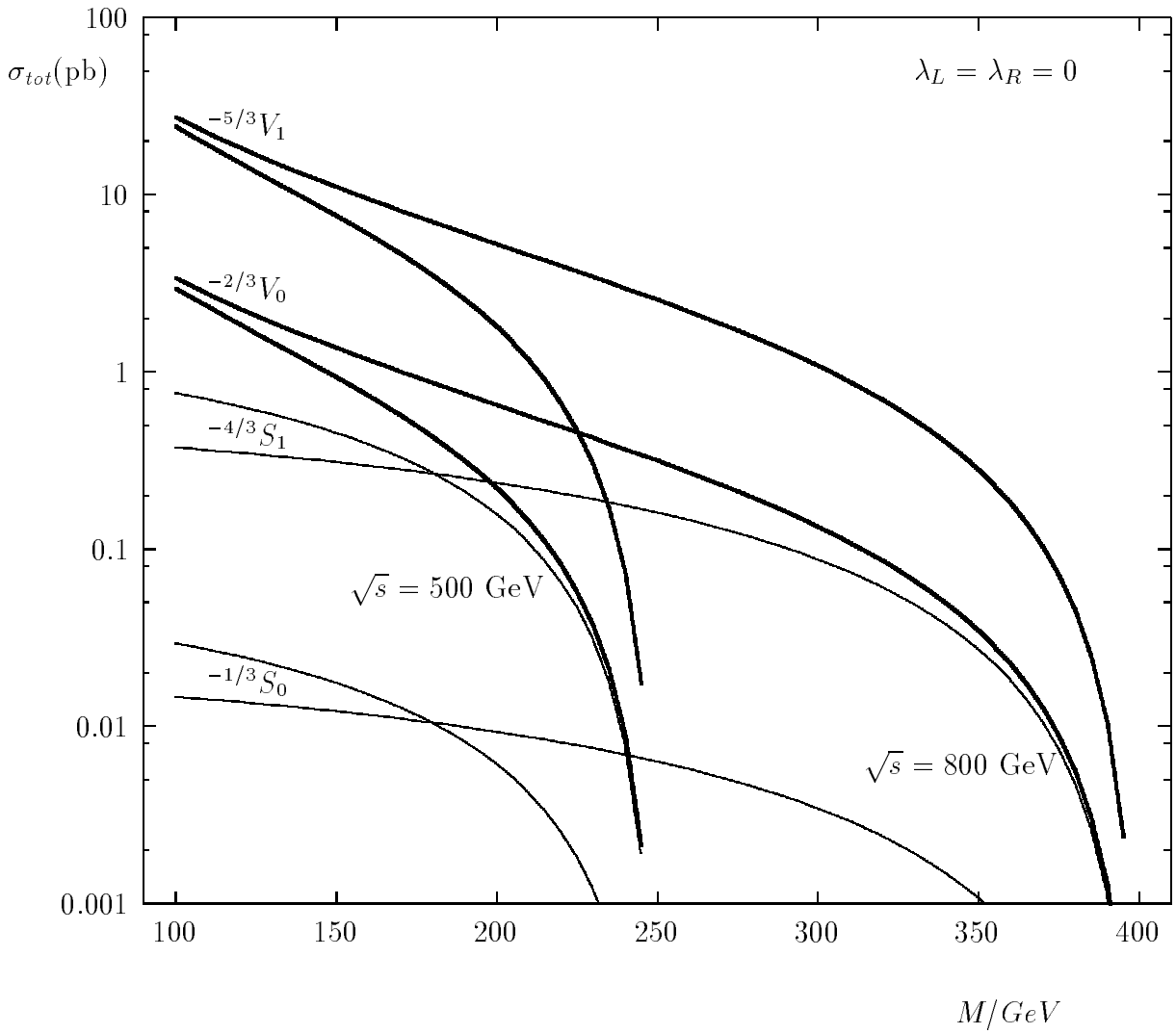

Figure 4: *Total cross sections for leptoquark pair-production at fixed center-of-mass energies as a function of the leptoquark mass M assuming vanishing Yukawa couplings and including corrections due to beamstrahlung and ISR.*

charged particles. In our calculations, the branching ratios are always taken for generic leptoquarks in accordance with the Yukawa couplings chosen in the production process. Of course, sufficiently small $\lambda_{L,R}$ has negligible influence on the production rates.

The formulae and prescriptions summarized in this section are implemented in the Monte Carlo event generator `LQPAIR`[3]. This program simulates production and decay of leptoquarks and is interfaced to parton shower and hadronization routines of `JETSET`. In the case of initial state radiation, events containing a bremsstrahlung photon are generated according to Eq. (15). The logarithm $\ln(4E^2/m_e^2)$ in Eq. (14) arises from the integration over transverse momenta of the emitted bremsstrahlung photon or, equivalently, over the

[3]The program was developed from an earlier generator `LQ2` by D. Gingrich [18]. The code is available from `http://www.desy.de/~hspiesb/lqpair.html`.

Isomultiplets	B_{eq}
$^{-1/3}S_0$ $^{-2/3}V_0$	$\dfrac{1+r}{2+r}$
$^{-4/3}\tilde{S}_0$ $^{-5/3}\tilde{V}_0$	1
$^{+2/3}S_1,\quad ^{-1/3}S_1,\quad ^{-4/3}S_1$ $^{+1/3}V_1,\quad ^{-2/3}V_1,\quad ^{-5/3}V_1$	$0,\ \dfrac{1}{2},\ 1$
$^{-2/3}S_{1/2},\quad ^{-5/3}S_{1/2}$ $^{-1/3}V_{1/2},\quad ^{-4/3}V_{1/2}$	$\dfrac{r}{1+r},\ 1$
$^{+1/3}\tilde{S}_{1/2},\quad ^{-2/3}\tilde{S}_{1/2}$ $^{+2/3}\tilde{V}_{1/2},\quad ^{-1/3}\tilde{V}_{1/2}$	$0,\ 1$

Table 3: *Branching ratios for charged lepton channels of generic leptoquarks ($r = \lambda_R^2/\lambda_L^2$).*

emission angle θ_γ of the photon with respect to the incoming electron (positron) beam:

$$\ln \frac{4E^2}{m_e^2} = \int_{-1}^{+1} d\cos\theta_\gamma \frac{E}{E - p\cos\theta_\gamma} \tag{17}$$

where $E \gg m_e$ is assumed. Therefore, transverse momenta are generated according to the integrand in Eq. (17).

3 Experimental Considerations

3.1 Detector Models

In addition to beam- and bremsstrahlung, we shall take into account detector effects such as limited acceptance and resolution. Geometrical acceptance cuts (beam hole) reduce the cross section, in particular in the forward and backward regions, which is important in cases where large t-channel contributions (due to large Yukawa couplings) are present. Furthermore, measurement uncertainties leading to a smearing of the lepton and hadron four-momenta deteriorate the reconstruction of jets and thus make the reconstruction of leptoquark masses less certain.

For our study we use two simple detector models interfaced to the leptoquark event generator. The main components are a tracking device and electromagnetic and hadronic calorimetry. Detector effects are described by Gaussian smearing of particle four-momenta. The single-particle detection efficiency is set to 98 % and the threshold energy to 0.3, 0.15,

and 0.6 GeV for electromagnetic particles, charged hadrons, and neutral hadrons, respectively. Table 4 lists the main detector parameters for the two models. A more detailed discussion of the detector models will be given elsewhere [19]. Our final results refer to the dedicated 1 TeV detector. In selected cases we also compare the latter with an LEP/SLC-type detector.

	1 TeV detector	LEP/SLC detector
Electromagnetic calorimeter $\frac{\sigma(E)}{E} = \frac{A_{\rm em}}{\sqrt{E}} + B_{\rm em}$	$A_{\rm em} = 0.10,\ B_{\rm em} = 0.01$	$A_{\rm em} = 0.20,\ B_{\rm em} = 0.01$
Hadronic calorimeter $\frac{\sigma(E)}{E} = \frac{A_{\rm had}}{\sqrt{E}} + B_{\rm had}$	$A_{\rm had} = 0.50,\ B_{\rm had} = 0.04$	$A_{\rm had} = 0.90,\ B_{\rm had} = 0.02$
Tracking (angular dependent) $\frac{\sigma(p_{x,y})}{p_{x,y}^2} = P_R$	$P_R(90^\circ) = 2 \cdot 10^{-4}$	$P_R(90^\circ) = 6 \cdot 10^{-4}$
Multiple scattering $\frac{\sigma(p_{x,y,z})}{p_{x,y,z}^2} = \frac{P_{MS}}{p_{x,y,z}\sqrt{\sin\theta}}$	$P_{MS} = 0.0015$	$P_{MS} = 0.0050$
Beam hole	8.1°	15°

Table 4: *Detector properties.*

3.2 Search Strategies

Leptoquarks decay into a lepton, either a charged one or a neutrino, and a quark which is observed as a jet of hadrons. Therefore the final states to be searched for are

$$\text{(I)}\quad \ell^+\ell^- + 2\text{jets}, \tag{18}$$

$$\text{(II)}\quad \ell^\pm + 2\text{jets} + p_{\rm miss}, \tag{19}$$

$$\text{(III)}\quad 2\text{jets} + p_{\rm miss} \tag{20}$$

where the lepton and quark flavors are assumed to belong to one given generation. We shall focus on the first generation, although most of our results should also hold for second generation leptoquarks.

Search I is straightforward. One has to identify two charged leptons in the event. The events should contain enough hadronic energy in order to allow the use of a jet algorithm to group the final state hadrons into two well-defined jets. Next, one combines one of the leptons with one of the jets. That combination which gives the smallest difference in the

invariant lepton-jet masses is accepted and the lepton-jet masses are associated with the leptoquark mass.

Search II requires the identification of events with one charged lepton, two jets, missing momentum and the determination of $p_{\rm miss}$. Assuming the observed missing momentum to be carried by one single neutrino, the event analysis can be performed in complete analogy to search I .

In search III, the signal is characterized by missing momentum and missing mass carried away by the unobserved neutrino pair. This is the most difficult case. Obviously, the measurements which can be carried out are not sufficient to reconstruct the leptoquark mass.

For clean event identification and precise mass reconstruction we require the following cuts on energies and transverse momenta in search I to III:

(I) two charged leptons with transverse momentum $p_T^l \geq 20$ GeV, missing transverse momentum $p_T^{miss} \leq 25$ GeV, two jets with energies $E_j \geq 10$ GeV, and total visible energy $E_{vis} \geq 0.9\sqrt{s}$;

(II) one, and only one, charged lepton with $p_T^l \geq 20$ GeV, $p_T^{miss} \geq 25$ GeV, two jets with $E_j \geq 10$ GeV, and $E_{vis} \geq 0.6\sqrt{s}$;

(III) no charged lepton with $p_T^l \geq 20$ GeV, $p_T^{miss} \geq 25$ GeV, two jets with transverse momentum $p_T^j \geq 75$ GeV each, and total hadronic energy $E_{had} \leq 300$ GeV. The upper limit on E_{had} corresponds to a lower limit for the missing mass of the neutrino pair.

These general requirements are supplemented by additional cuts to suppress the background processes which are discussed in the next subsection.

3.3 Background Processes

Vector boson pair-production is an obvious source of final states of the kind Eqs. (18) to (20) within the standard model:

$$e^+e^- \to ZZ, \tag{21}$$

$$e^+e^- \to W^+W^- \tag{22}$$

with one Z (W) decaying into a lepton pair and the other one into two jets. More generally, one has to consider four-fermion production

$$e^+e^- \to l_1\bar{l}_2q_3\bar{q}_4 \tag{23}$$

comprising also single-resonant processes like $e^+e^- \to Z\nu\nu, Z\ell\ell, W\ell\nu$ with $Z \to q\bar{q}$ and $W \to q_1\bar{q}_2$, as well as completely non-resonant processes. Whereas on-shell W and Z production can be suppressed efficiently by rejecting events with pairs of final state leptons

or jets having a mass close to M_W or M_Z, suppression of off-shell production requires additional cuts. We implement them as cuts on the various invariant masses $M_{l_i j_k}$.

Apart from the irreducible background due to final states containing the same particles as the signal events, there is in addition some reducible background due to processes with the same visible particles produced by different final states. In particular, b-quarks and τ-leptons have some probability to produce final states with an energetic electron, that may mimic the decay products of a leptoquark.

A second important source of background is $t\bar{t}$ production:

$$e^+e^- \to t\bar{t} \tag{24}$$

with the top-quarks decaying into b and W and the latter decaying leptonically.

The cuts devised to suppress these background processes are summarized below. The indices j_1 and j_2 label the two jets ordered by their energies, i.e., $E_{j_1} > E_{j_2}$. l_1 and l_2 denote the leptons ordered in such a way that

$$|M_{l_1 j_1} - M_{l_2 j_2}| < |M_{l_1 j_2} - M_{l_2 j_1}| \,. \tag{25}$$

With this convention, the pairs $l_1 j_1$ and $l_2 j_2$ are candidates for the decay products of a leptoquark. In search (I) to (III) we require:

(I) $|M_{l_1 l_2} - M_Z| \geq 10$ GeV and $|M_{j_1 j_2} - M_{W,Z}| \geq 10$ GeV;
$M_{l_1 l_2} \geq 20$ GeV, $M_{l_1 j_2} \geq 20$ GeV, $M_{l_2 j_1} \geq 20$ GeV.

(II) $|M_{l_1 l_2} - M_W| \geq 20$ GeV and $|M_{j_1 j_2} - M_{W,Z}| \geq 20$ GeV;
$M_{l_1 l_2} \geq 20$ GeV, $M_{l_1 j_2} \geq 20$ GeV, $M_{l_2 j_1} \geq 20$ GeV;
$E_{had} \geq 150$ GeV.

(III) $|M_{l_1 l_2} - M_Z| \geq 20$ GeV and $|M_{j_1 j_2} - M_{W,Z}| \geq 20$ GeV;
$M_{j_1 j_2} \leq 400$ GeV.

Table 5 indicates the number of remaining events from various reducible and irreducible background processes. The estimates for four-fermion final states have been obtained with the help of `WPHACT` [20], those for $t\bar{t}$ production with `PYTHIA` [21]. Beamstrahlung and ISR are not included here. These corrections should be negligible for the present purpose.

In search I, the dominant background is due to on- and off-shell boson pair-production with $e^\pm$ in the final state, i.e., $e^+e^- \to e^+e^- q\bar{q}$ and $e^+e^- \to e^\pm \nu q\bar{q}'$. The rate is much higher than at LEP2 energies estimated in a previous study of leptoquark production [22]. Whereas $t\bar{t}$ production is not a problem for search I, it makes the search for leptoquarks in channel II very difficult. In search III, the number of background events surviving the cuts is very large, since the final state cannot be reconstructed completely. In particular, final states with b-quarks and τ's contribute a large fraction. It seems unlikely that in this channel one can expect more than a consistency check of the searches I and II.

Due to their huge cross sections, two-photon processes have also to be considered as a potential source of background although four-fermion final states only emerge at higher orders. We checked for a sample of $2 \cdot 10^5$ $\gamma\gamma$ events generated with the help of the event generator `PYTHIA` (version 5.722) that no event passed the cuts for searches I and II, whereas in search III a negligibly small number of events remained.

	$\sqrt{s} = 500$ GeV $\mathcal{L} = 20$ fb^{-1}			$\sqrt{s} = 800$ GeV $\mathcal{L} = 50$ fb^{-1}		
source	I	II	III	I	II	III
$e^+e^-q\bar{q},\ q = u,d,s,c,b$ $e^-\nu_e\bar{u}d$ + c.c. $e^-\nu_e\bar{c}s$ + c.c.	11.9	14.8	266	15.0	39.3	1550
$b\bar{b}f\bar{f},\ f \neq e$	–	1.4	495	–	1.3	2410
$\tau^+\tau^- f\bar{f},\ f \neq b$ $\tau^{\pm}\ \overset{(-)}{\nu}_{\tau}\ q\bar{q}'$	0.4	1.3	888	0.6	5.1	320
other 4f	–	0.1	371	–	8.0	1250
sum of 4f	12.3	17.6	2010	15.6	53.7	5540
$t\bar{t}$	0.7	132	527	1.5	91.6	97.8
total	13.0	150	2537	17.1	145.3	5630

Table 5: *Number of background events surviving the cuts in the leptoquark searches (I) to (III) at $\sqrt{s} = 500$ GeV ($\mathcal{L} = 20$ fb^{-1}) and 800 GeV ($\mathcal{L} = 50$ fb^{-1}).*

4 Results

In the following, we restrict ourselves to generic leptoquarks of the first generation which decay into $e^{\pm}$ or ν_e and a jet. Except where stated differently we assume

$$\lambda_L \ll 1, \qquad \lambda_R \ll 1, \tag{26}$$

so that the Yukawa couplings have negligible effects on the production cross sections. Note that in this case the production rates are actually independent of the generation quantum number. However, the decay products of third generation leptoquarks contain the heavy flavors τ, b and t which in turn decay into lighter leptons and jets. Hence, the search strategies explained in section 3 are not appropriate.

4.1 Signal Distributions

Figure 5 illustrates some characteristic distributions generated from the class II process $e^+e^- \to {}^{-1/3}S_1 + {}^{1/3}\bar{S}_1 \to e^{\pm}\ \overset{(-)}{\nu}_e\ jj$ for $M = 250$ GeV and $\sqrt{s} = 800$ GeV in a high

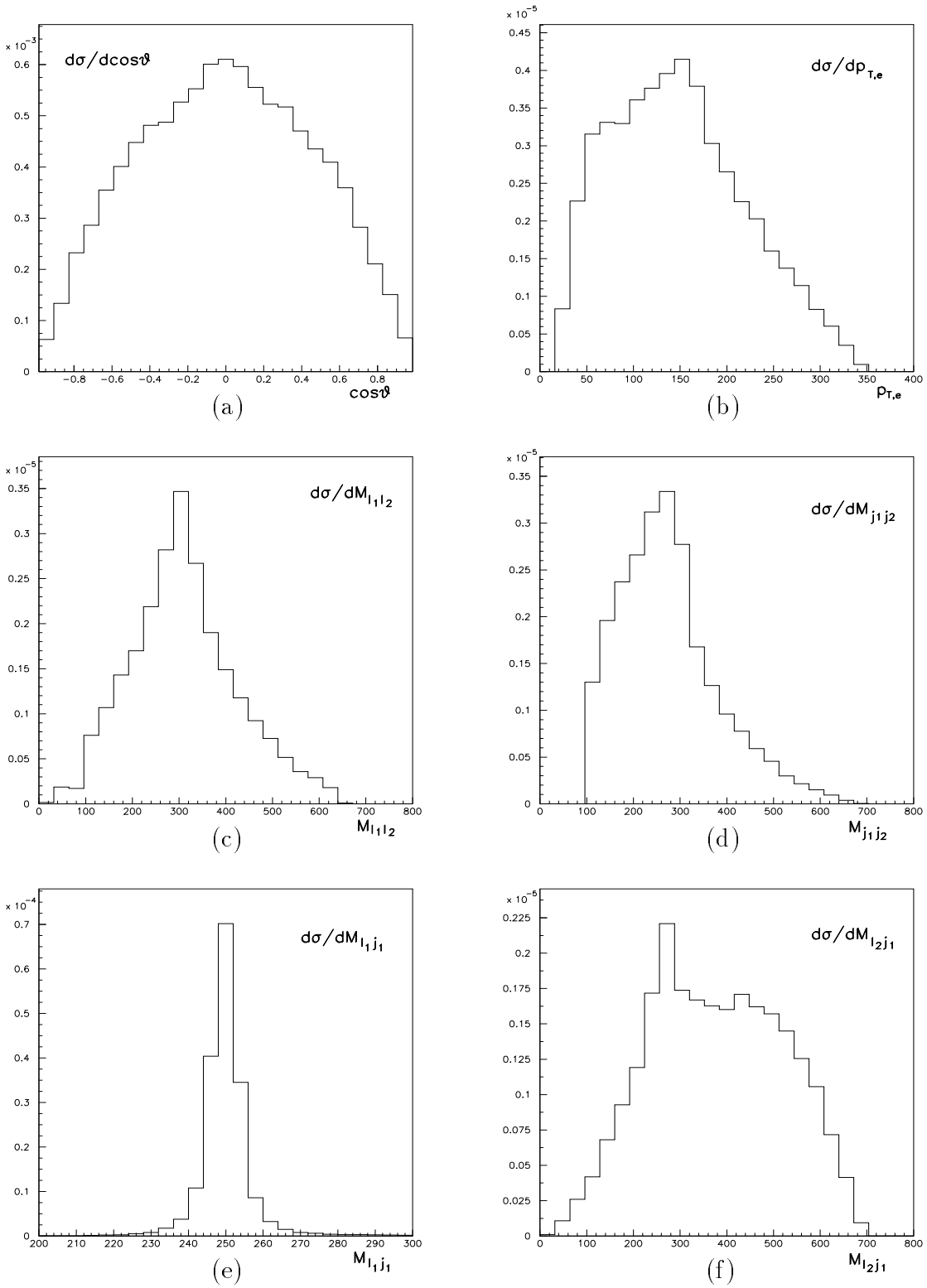

Figure 5: *Event distributions for the process* $e^+e^- \to {}^{-1/3}S_1 + {}^{1/3}\bar{S}_1 \to e^{\pm} \overset{(-)}{\nu}_e jj$ *for* $M = 250$ *GeV at* $\sqrt{s} = 800$ *GeV (search II). Masses are given in GeV and cross sections in pb. The definition of kinematic variables is explained in subsection 3.3.*

statistics Monte Carlo run. Beamstrahlung, ISR, detector effects and cuts are taken into account as described above. In Fig. 5a one sees the $\sin^2\theta$-distribution characteristic for the production of scalar particles which can nicely be reconstructed under the given assumptions. Figure 5b displays the distribution in the transverse momentum of the decay electron (positron), which is practically the same for the missing transverse momentum and the jet transverse momentum. The invariant-mass distributions of the lepton and the jet pairs shown in Figs. 5c and 5d have their maximum at about 300 GeV, while the leptoquark signal is clearly visible in the distribution of $M_{l_1 j_1}$ of Fig. 5e. The tails in this distribution extending to smaller and higher masses are small. From Fig. 5f we see that the identification of the correct combination of leptons and jets is not perfect: the mass distribution of the 'wrong' combination shows some excess of events in the region of $M_{l_2 j_1} \simeq 250$ GeV $= M$.

4.2 Detection Efficiencies

The cuts described in subsections 3.2 and 3.3 are considered a reasonable compromise between the two conflicting requirements of background suppression and preservation of the signal rate. It is certainly possible to further optimize them. Particularly worthwhile may be some fine-tuning for different ranges of center-of-mass energies and leptoquark masses.

Table 6 gives an overview of the potential in the leptoquark searches I and II. Column 2 displays the number of events observed divided by the respective branching ratios $B_I = B_{eq}^2$ and $B_{II} = 2B_{eq}B_{\nu q}$ or, equivalently, the number of leptoquarks produced and surviving the cuts in channel I and II, respectively. One can see that in both cases the signal efficiency is reasonably large, between 20 % and 40 %. There is no significant difference in the efficiencies for scalar and vector leptoquarks. Furthermore, we find that for a LEP/SLD-type detector the reconstruction efficiency is lower by typically 20 % relative to the dedicated 1 TeV detector, depending on the channel and the leptoquark mass. This reduction originates mainly from the different size of the beam-holes (see Table 4).

The results in Table 6 are obtained for negligibly small Yukawa couplings, i.e., for leptoquarks with very small natural widths (see Eq. (16)). Beamstrahlung, initial state radiation, and in particular hadronization effects lead to a considerable broadening of the observed leptoquark mass distribution. In order to estimate the mass resolution, we fitted the reconstructed mass distribution to a Gaussian. Column 4 of the table shows the standard deviation of such a fit. Note that the precision with which the peak position of the reconstructed mass distribution can be determined is, in most cases, better by a factor of 5 to 10, i.e., $\delta M = 0.5$ to 0.8 GeV. From column 4 and Eq. (16) one clearly sees that a measurement of the mass distribution of leptoquark decay products will not allow to determine the intrinsic leptoquark width for accessible masses and values of $\lambda_{L,R}$ allowed by the existing bounds.

Finally, Table 6 reveals a systematic shift of the reconstructed leptoquark mass. Again, this is dominantly due to hadronization effects and depends strongly on the algorithm used

I $M = 225$ GeV $\sqrt{s} = 500$ GeV	number of events N_{events}/B_I ($\mathcal{L} = 20$ fb^{-1})	signal efficiency (%)	standard deviation (GeV)	mass shift (GeV)
$^{-1/3}S_0$	9 / 8	26.5 / 23.8	4.8 / 5.9	-3.0 / -3.1
$^{-4/3}S_1$	259 / 220	27.2 / 23.1	5.0 / 5.9	-2.9 / -3.3
$^{-2/3}V_0$	313 / 269	27.2 / 23.4	5.0 / 5.9	-3.0 / -3.2
$^{-5/3}V_1$	2640 / 2300	28.1 / 24.5	4.5 / 5.8	-2.9 / -3.2
I $M = 350$ GeV $\sqrt{s} = 800$ GeV	N_{events}/B_I ($\mathcal{L} = 50$ fb^{-1})			
$^{-1/3}S_0$	19 / 15	36.8 / 28.7	5.1 / 6.6	-3.3 / -4.2
$^{-4/3}S_1$	492 / 378	35.9 / 27.8	5.2 / 6.8	-3.2 / -4.2
$^{-2/3}V_0$	608 / 486	35.1 / 28.1	5.2 / 6.6	-3.2 / -4.4
$^{-5/3}V_1$	5080 / 3780	36.3 / 27.0	5.1 / 6.6	-3.3 / -4.1
II $M = 225$ GeV $\sqrt{s} = 500$ GeV	N_{events}/B_{II} ($\mathcal{L} = 20$ fb^{-1})			
$^{-1/3}S_0$	8 / 7	24.0 / 19.5	6.5 / 8.0	$+1.3$ / $+1.6$
$^{-2/3}V_0$	269 / 234	23.4 / 20.4	6.7 / 7.3	$+1.6$ / $+0.9$
II $M = 350$ GeV $\sqrt{s} = 800$ GeV	N_{events}/B_{II} ($\mathcal{L} = 50$ fb^{-1})			
$^{-1/3}S_0$	16 / 12	29.7 / 23.3	5.9 / 6.7	-0.8 / -1.3
$^{-2/3}V_0$	488 / 397	28.2 / 23.0	5.8 / 6.9	-0.7 / -1.5

Table 6: *Event number, signal efficiency, difference in reconstructed and nominal leptoquark mass, and width of the reconstructed mass peak for two scenarios and in two search channels. The expected numbers of events in column 2 are divided by the respective branching ratios $B_I = B_{eq}^2$, $B_{II} = 2B_{eq}B_{\nu q}$. The first number given in each column refers to a dedicated 1 TeV detector, the second one to a LEP/SLC-type detector.*

for jet reconstruction (see for example [23]). We compared the JADE and Durham schemes with E, E0, P, and P0 recombination and found that the Durham-P scheme leads to the smallest mass shifts. Other jet algorithms induce considerably larger shifts, for example, the JADE-E scheme a shift up to 10 GeV. Therefore, the Durham-P algorithm was used in the subsequent analysis.

In channel III, no mass reconstruction is possible. The signal efficiency ranges from 40 to 45 % at $\sqrt{s} = 500$ GeV and from 7 to 15 % at $\sqrt{s} = 800$ GeV.

4.3 Sensitivity Limits

From the above it becomes clear that the discovery potential in the three channels is very different. In other words, for a given leptoquark species, the observability strongly depends on the branching ratio for the decay into a charged lepton, here $e^{\pm}$. As can be seen from Table 3, this branching ratio is fixed for all states with the exception of ${}^{-1/3}S_0$, ${}^{-2/3}V_0$, ${}^{-2/3}S_{1/2}$, and ${}^{-1/3}V_{1/2}$. In the latter cases, the branching ratio is determined by the ratio $r = \lambda_R^2/\lambda_L^2$. Below we shall present results for $r = 0, 1$ and ∞, corresponding to $B_{eq} = 1/2$, $2/3$, and 1.

A first estimate of the sensitivity limits can be based on the total number of events. Requiring a 5σ effect, we determine the values of M for which the number of signal events is equal to or larger than $5\sqrt{N_{bg}}$ where N_{bg} is the total number of background events. This is a sensible discovery criterion for search I where the number of background events is small. The results are collected in Table 7 for all leptoquark species of Table 1. In search I, scalar leptoquarks can be discovered for masses between 80 and 97 % of $\sqrt{s}/2$ except for the states ${}^{-1/3}S_0$ and ${}^{-1/3}S_1$ where only 70 % of $\sqrt{s}/2$ can be reached for purely left-handed couplings. For vector leptoquarks the mass reach is always larger than 95 % of $\sqrt{s}/2$. In searches II and III, the discovery limits are worse. In these channels, some scalars cannot be detected at all for masses above 100 GeV. It should also be noted that small, but non-negligible Yukawa couplings [13] and anomalous couplings [14] can lower the production cross sections and discovery limits in comparison to Table 7.

A more refined analysis is possible if the number of events is sufficiently large to investigate the mass distributions. The signal is expected to stick out as a prominent peak over a flat background distribution. From an investigation of the mass distribution one would obtain a higher significance for leptoquarks with the masses shown in Table 7 than the global 5σ assumed there. This is demonstrated in Fig. 6a for a favorable case, while Fig. 6b illustrates a more difficult situation. In the latter, the 9 signal events expected for $M = 200$ GeV disappear in the $t\bar{t}$ background, whereas the 33 signal events for $M = 160$ GeV might still allow to identify an enhancement in the mass distribution. This, however, requires a mass resolution better than 5 GeV.

Note that for Fig. 6 we have assumed $\lambda_L = \lambda_R \ll 1$. Vanishing λ_L forbids class II final states. For ${}^{-2/3}S_{1/2}$ (Fig. 6a) this is also the case for $\lambda_R = 0$, while for ${}^{-1/2}S_0$ the signal distributions shown in Fig. 6b have to be rescaled by the factor 8/9. For small, but non-negligible Yukawa couplings, the production rates may be either enhanced or reduced relative to the case of negligible $\lambda_{L,R}$, whereas for sufficiently large couplings the t-channel contribution always leads to larger cross sections[4].

4.4 Leptoquark Couplings

Assuming that the masses are known and the Yukawa couplings not too large, different species of leptoquarks can be distinguished already by their total production cross section

[4]The influence of anomalous couplings is discussed in Ref. [14].

		$\sqrt{s}=500$ GeV			$\sqrt{s}=800$ GeV		
Search		I	II	III	I	II	III
$5\sqrt{N_{bg}}$		18	61	251	21	60	375
States	B_{eq}	Mass reach in GeV					
$^{-1/3}S_0$	2/3	202	*	*	318	*	*
	1/2	183	*	*	289	*	*
	1	217	–	–	350	–	–
$^{-4/3}\tilde{S}_0$	1	242	–	–	387	–	–
$^{2/3}S_1$	0	–	–	225	–	–	275
$^{-1/3}S_1$	1/2	183	*	*	289	*	*
$^{-4/3}S_1$	1	244	–	–	389	–	–
$^{-2/3}S_{1/2}$	1/2	230	221	179	369	359	*
	0	–	–	218	–	–	239
	1	240	–	–	384	–	–
$^{-5/3}S_{1/2}$	1	244	–	–	389	–	–
$^{1/3}\tilde{S}_{1/2}$	0	–	–	198	–	–	146
$^{-2/3}\tilde{S}_{1/2}$	1	237	–	–	379	–	–
$^{-1/3}V_{1/2}$	1/2	241	237	220	385	380	266
	0	–	–	236	–	–	326
	1	245	–	–	392	–	–
$^{-4/3}V_{1/2}$	1	247	–	–	395	–	–
$^{2/3}\tilde{V}_{1/2}$	0	–	–	236	–	–	326
$^{-1/3}\tilde{V}_{1/2}$	1	244	–	–	390	–	–
$^{-2/3}V_0$	2/3	241	233	195	385	373	200
	1/2	238	234	212	380	376	244
	1	244	–	–	390	–	–
$^{-5/3}\tilde{V}_0$	1	247	–	–	396	–	–
$^{1/3}V_1$	0	–	–	241	–	–	352
$^{-2/3}V_1$	1/2	238	234	212	380	375	244
$^{-5/3}V_1$	1	248	–	–	396	–	–

Table 7: *Discovery limits for leptoquarks (masses in GeV) at* $\sqrt{s}=500$ *GeV* ($\mathcal{L}=20$ *fb*$^{-1}$) *and* $\sqrt{s}=800$ *GeV* ($\mathcal{L}=50$ *fb*$^{-1}$) *requiring a* 5σ *effect. Dashes indicate cases where the corresponding search is not possible,* $*$ *means no sensitivity to masses above 100 GeV with the cuts considered.*

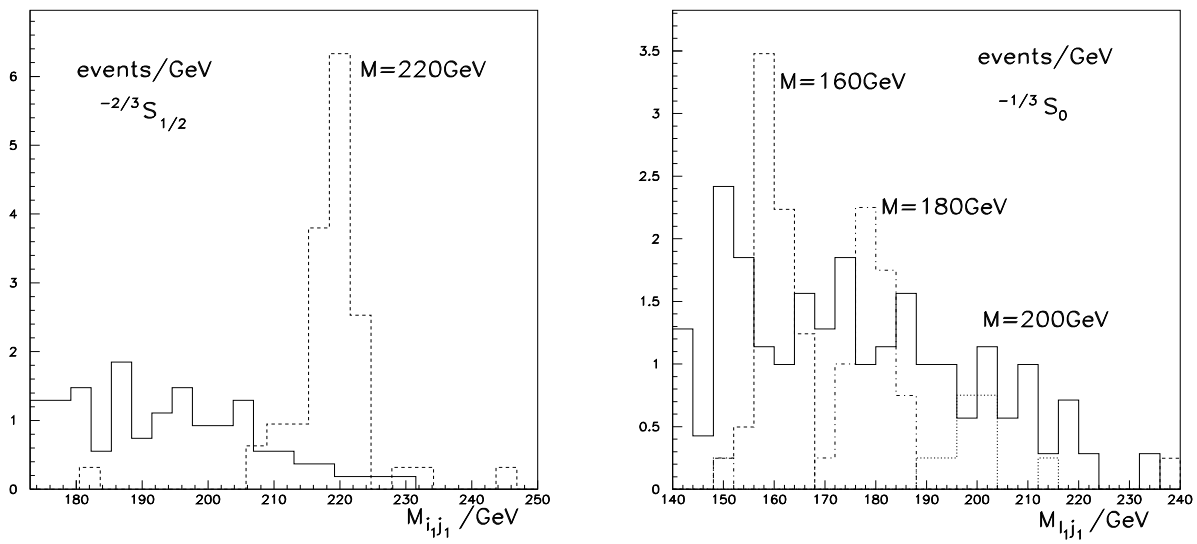

Figure 6: *Signal and background distributions in the invariant mass $M_{l_1j_1}$ for the channel $e^{\pm}\nu$+2jets and $\sqrt{s} = 500$ GeV, $\mathcal{L} = 20$ fb^{-1}: (a) $^{-2/3}S_{1/2}$ production, (b) $^{-1/3}S_0$ production and $M = 160$ GeV (dashed), $M = 180$ GeV (dash-dotted) and $M = 200$ GeV (dotted). The full histograms show the dominant background from $t\bar{t}$ production.*

(see Fig. 4 and Table 1). The angular distribution gives an additional handle on the spin and the relative size of the couplings to gauge bosons and fermions. For most of the leptoquarks in Table 1 the s/t-channel interference is destructive reducing the cross section in the central region. By contrast, the pure t-channel contribution increases the cross section in the forward region. However, the Yukawa couplings have to be relatively large to make this an observable effect. In Fig. 7 the differential cross sections[5] $d\sigma/d\theta$ including all cuts, beamstrahlung and ISR are shown for $^{-4/3}S_1$ and $^{-2/3}V_0$ which have comparable production cross sections (see Table 1). From the angular distribution it should not be difficult to distinguish scalars from vectors, but the shape of the distributions does not reflect the presence and size of Yukawa couplings as clearly as one would wish.

Another difficulty follows from the fact that, in general, the detection efficiencies have an angular dependence which distorts the observable distributions, in particular in the forward and backward regions. Figure 8 illustrates the angular dependence of the detection efficiencies. For scalars (Fig. 8a) the cross section vanishes in the forward and backward region, leading to large statistical fluctuations. Hence, detector effects show up mainly in the normalization of the cross sections. However, for vector leptoquarks (Fig. 8b), the efficiency decreases by almost 30 % at small and large angles. This demands a precise unfolding of the efficiency, before one can hope to probe the Yukawa couplings.

In order to evaluate the prospects for determining the couplings of scalars more quantitatively, we have fitted the measured angular distribution to the differential cross section

[5]Here, charge identification of the decay leptons is essential in order to remove the sign ambiguity of $\cos\theta$. Experimentally this is possible for searches I and II even for very energetic electrons/positrons.

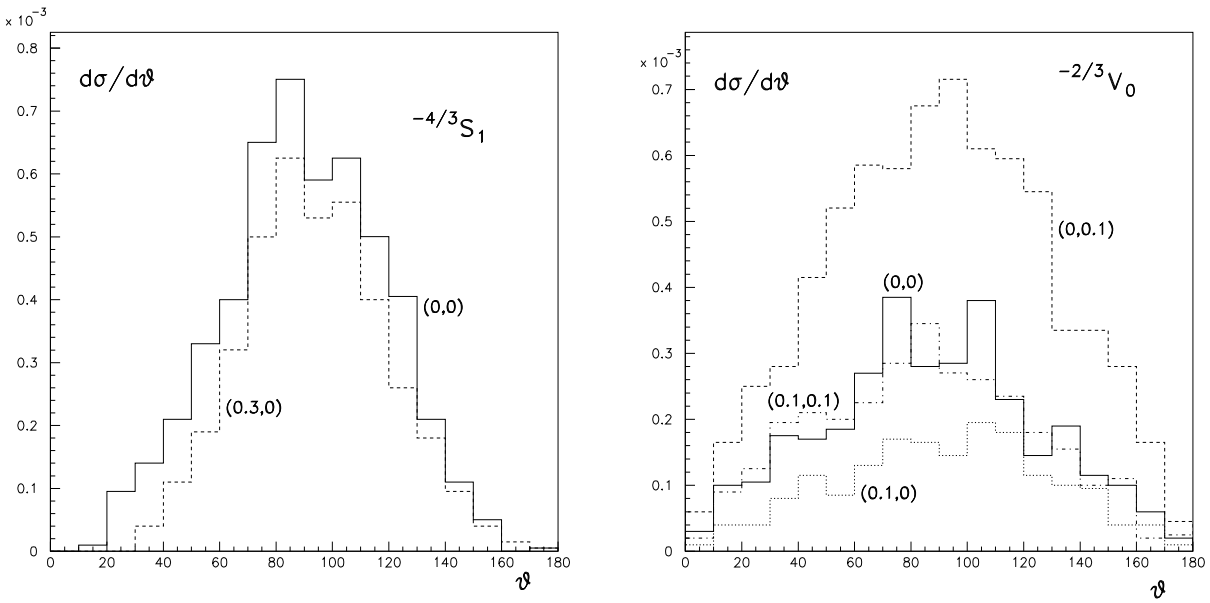

Figure 7: *Angular dependence of the production cross sections for (a) $^{-4/3}S_1$ and (b) $^{-2/3}V_0$ for various Yukawa couplings (g_L, g_R) in units of e ($M = 300$ GeV, $\sqrt{s} = 800$ GeV, $\mathcal{L} = 50 fb^{-1}$, cuts included).*

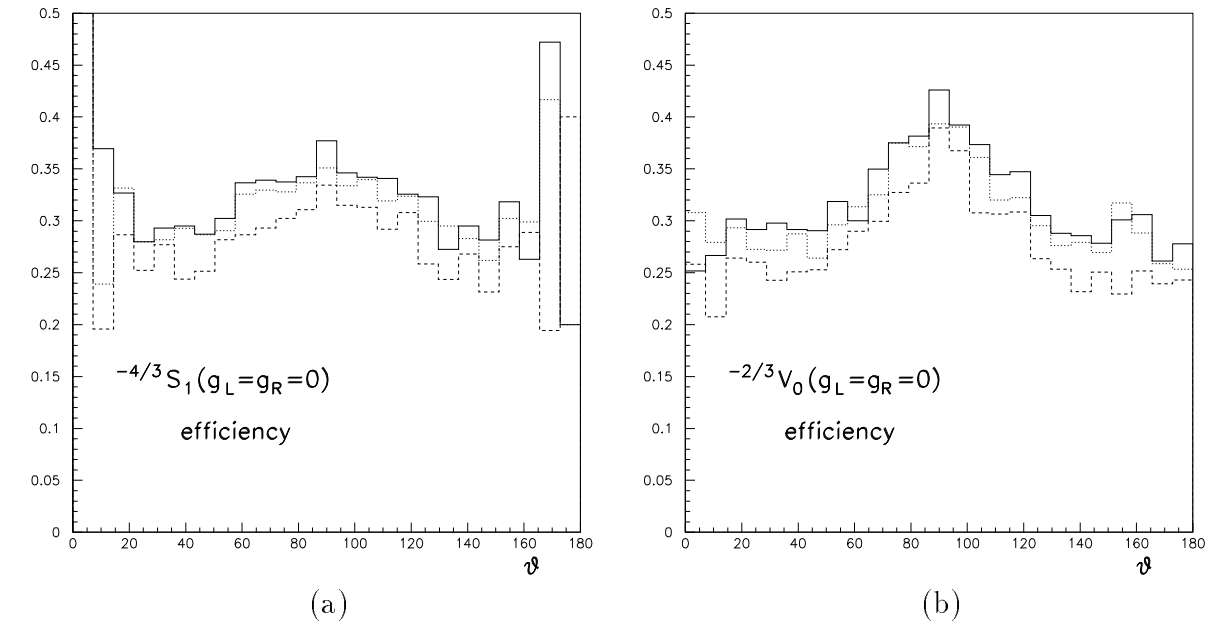

Figure 8: *Angular dependence of the detection efficiency for a scalar (a) and a vector (b) leptoquark in channel I. The full histogram refers to the 1 TeV detector, the dashed one to a LEP/SLD-type detector. The dotted histogram is obtained with the detector simulation of Ref. [24].*

$d\hat{\sigma}/d\cos\theta$ given in Eq. (5) with the normalization as a free parameter. Consequently, one can only determine ratios of the effective coupling parameters g_1, g_2, and g_3, defined in Eqs. (6 - 8). Taking $M = 200$ GeV, $\sqrt{s} = 500$ GeV and $\mathcal{L} = 20\text{fb}^{-1}$, it turns out that for $|g_2/g_1| > 0.5$ and $g_3/g_1 > 0.15$ the ratios g_2/g_1 and g_3/g_1 can be determined to 10 % accuracy. The above ranges correspond to Yukawa couplings $\lambda_{L,R}$ between 0.2 and 0.6 (note that the relation between the g_i and $\lambda_{L,R}$ depends on the leptoquark quantum numbers). This result does not change strongly with s and M. For $\lambda_{L,R} < 0.1$, the range allowed by low-energy data (see Table 1), it seems to be difficult to probe the Yukawa couplings by investigating the angular distributions.

5 Conclusions

Linear e^+e^- colliders provide unique tools to search for leptoquarks independently of the size of their Yukawa couplings to lepton-quark pairs. The relatively clean environment of e^+e^- annihilation allows to reconstruct leptoquark masses from the decay products also in the presence of beamstrahlung, QED initial state radiation, and hadronization effects. The discovery limits depend on the quantum numbers of the particular leptoquark and are estimated to reach $M = (0.9 \text{ to } 0.95)\sqrt{s}/2$ in the most favorable cases.

The masses can be reconstructed with a precision of 0.5 to 0.8 GeV assuming the detector performance expected for a dedicated 1 TeV detector and not accounting for systematic mass shifts. Past experience at LEP has shown that for the analysis of real data better measuring accuracies can be achieved relative to early simulations. Measurements of the total cross sections in combination with an analysis of the angular distributions will allow to clearly distinguish scalar from vector leptoquarks. Yukawa couplings can be determined probably only if they are of a strength comparable to the electromagnetic coupling.

In summary, searches for leptoquarks at e^+e^- linear colliders are complementary to pp collisions which also probe the existence of these novel states independently of the unknown Yukawa couplings, but with less power in distinguishing states with different quantum numbers. On the other hand, Yukawa couplings can be probed by searching for virtual leptoquark effects in $e^+e^- \to q\bar{q}$ and $pp \to e^+e^-$, and most efficiently in ep collisions.

References

[1] W. Buchmüller R. Rückl and D. Wyler, Phys. Lett. B191 (1987) 442.

[2] B. Abbott et al., D0 Collaboration, FERMILAB-PUB-97/252-E (hep-ex/9707033).

[3] F. Abe et al., CDF Collaboration, FERMILAB-PUB-97/280-E.

[4] J. A. Valls, FERMILAB-CONF-97/135-E, XXXII Rencontres de Moriond, QCD and Hadronic Interactions, Les Arcs, France, 1997; G. Landsberg, Fermilab Seminar, June 6, 1997, `http://d0sgi0.fnal.gov/public/new/analyses/lq/lq_jun97.html`.

[5] F. Abe et al., CDF Collaboration, Phys. Rev. Lett. 78 (1997) 2906 and Phys. Rev. Lett. 75 (1995) 1012; B. Abbott et al., D0 Collaboration, paper 109 submitted to the International Europhysics Conference on High Energy Physics, Jerusalem, 1997.

[6] S. Aid et al., H1 Collaboration, Phys. Lett. B369 (1996) 173; M. Derrick et al., ZEUS Collaboration, Phys. Lett. B306 (1993) 173 and Z. Phys. C73 (1997) 613.

[7] OPAL Collaboration, OPAL Physics Note 288, paper LP138 submitted to the XVIII International Symposium on Lepton-Photon Interactions, Hamburg, 1997.

[8] B. Adeva et al., L3 Collaboration, Phys. Lett. B261 (1991) 169; G. Alexander et al., OPAL Collaboration, Phys. Lett. B263 (1991) 123; P. Abreu et al., DELPHI Collaboration, Phys. Lett. B316 (1993) 620.

[9] S. Davidson et al., Z. Phys. C61 (1994) 613; M. Leurer, Phys. Rev. D49 (1994) 333 and D50 (1994) 536.

[10] J. Kalinowski, R. Rückl, H. Spiesberger and P. M. Zerwas, Z. Phys. C74 (1997) 595.

[11] J. L. Hewett and T. G. Rizzo, Phys. Rev. D36 (1987) 3367; D. Schaile and P. M. Zerwas, Proceedings, *Physics at Future Accelerators* (La Thuile, Geneva 1987), ed. J. H. Mulvey, CERN 87-07; N. D. Tracas and S. D. P. Vlassopulos, Phys. Lett. B220 (1989) 285; A. Djouadi, M. Spira and P. M. Zerwas, Proceedings, e^+e^- *Collisions at 500 GeV: The Physics Potential* (Munich, Annecy, Hamburg 1991), ed. P. M. Zerwas, DESY 92-123B; J. Blümlein and R. Rückl, *ibid.*; J. E. Cieza Montalvo and O. J. P. Éboli, Phys. Rev. D47 (1993) 837; J. Blümlein and R. Rückl, Phys. Lett. B304 (1993) 337; D. Choudhury, Phys. Lett. B346 (1995) 291; O. J. P. Éboli, M. C. Gonzalez-Garcia and J. K. Mizukoshi, Phys. Lett. B396 (1997) 238; J. L. Hewett and T. G. Rizzo, SLAC-PUB-7430 (hep-ph/9703337).

[12] B. Schrempp, *Leptoquarks and Leptogluons at HERA – Theoretical Perspectives*, Proceedings of the Workshop *Physics at HERA*, Hamburg, 1991, eds. W. Buchmüller and G. Ingelman, Vol. 2, p. 1034.

[13] J. Blümlein and R. Rückl, Phys. Lett. B 304 (1993) 337.

[14] J. Blümlein, E. Boos and A. Kryukov, Phys. Lett. B392 (1997) 150.

[15] T. Ohl, Comput. Phys. Commun. 101 (1997) 269.

[16] F. Jegerlehner, Proceedings of the Workshop *QCD and QED in Higher Orders*, Rheinsberg, Germany, 1996, Nucl. Phys. Proc. Suppl. 51C (1996) 131.

[17] J. Schwinger, Particles, Sources and Fields, Vol. II, p. 397, Addison-Wesley, Reading, MA, 1989; M. Drees and K. Hikasa, Phys. Lett. B252 (1990) 127.

[18] D. M. Gingrich, *Monte Carlo Generator for Leptoquark Production in Lepton-Proton Collisions*, Oxford University preprint OUNP-92-19; M. L. Mangano et al., *Event Generators for Discovery Physics*, LEP-2 report, CERN, 1996 (hep-ph/9602203); D. Gingrich and N. Harnew, *Monte Carlo Generator for Leptoquark Production in Lepton-Proton Collisions*, Proceedings of the Workshop *Physics at HERA*, Hamburg, 1991, eds. W. Buchmüller and G. Ingelman, Vol. 3, p. 1542.

[19] R. Settles, H. Spiesberger and W. Wiedenmann, `SMEAR, v.3.02`, `http://www.desy.de/~hspiesb/smear.html`.

[20] E. Accomando and A. Ballestrero, Comput. Phys. Commun. 99 (1997) 270.

[21] H.-U. Bengtsson and T. Sjöstrand, Comput. Phys. Commun. 46 (1987) 43; T. Sjöstrand, Comput. Phys. Commun. 82 (1994) 74; T. Sjöstrand, LU TP 95-20 and CERN-TH.7112/93 (revised Aug. 1995).

[22] G. F. Giudice et al., Proceedings of the Workshop on Physics at LEP2, Geneva, 1996, eds. G. Altarelli, T. Sjöstrand and F. Zwirner, CERN report 96-01, Vol. 1, p. 463.

[23] S. Bethke, Z. Kunszt, D. E. Soper and W. J. Stirling, Nucl. Phys. B370 (1992) 310.

[24] J. Schreiber, `SIMDET`, program for detector smearing, private communication.